Human Molecular Genetics, 2011, Vol. 20, No. 18 **3642–3652**
doi:10.1093/hmg/ddr284
Advance Access published on June 17, 2011

Downregulation of VAPB expression in motor neurons derived from induced pluripotent stem cells of ALS8 patients

Miguel Mitne-Neto[1,2], Marcela Machado-Costa[3], Maria C.N. Marchetto[4], Mario H. Bengtson[5], Claudio A. Joazeiro[5], Hiroshi Tsuda[6], Hugo J. Bellen[6], Helga C.A. Silva[3], Acary S.B. Oliveira[3], Monize Lazar[2], Alysson R. Muotri[1,*] and Mayana Zatz[2,*]

[1]University of California San Diego, School of Medicine, Department of Pediatrics/Rady Children's Hospital San Diego, Department of Cellular & Molecular Medicine, Stem Cell Program, 9500 Gilman Dr, La Jolla, CA 92093, MC 0695, USA, [2]Department of Genetics and Evolutive Biology, Human Genome Research Center, University of São Paulo, Rua do Matão, 106 - Cidade Universitária, 05508-090 São Paulo, SP, Brazil, [3]Paulista School of Medicine, Federal University of São Paulo, Rua Botucatu, 740, Vila Mariana, São Paulo, SP, Brazil, [4]Laboratory of Genetics, The Salk Institute for Biological Studies, 10010 North Torrey Pines Road, La Jolla, CA 92037, USA, [5]Department of Cell Biology, The Scripps Research Institute, CB168, 10550 North Torrey Pines Road, La Jolla, CA 92037, USA, [6]Department of Molecular and Human Genetics and Program in Developmental Biology-Baylor College of Medicine-Jan and Dan Duncan Neurological Research Institute, 1250 Moursund St. Suite 1125, Mailstop NR-1125, Houston, TX 77030, USA

Received March 11, 2011; Revised May 22, 2011; Accepted June 13, 2011

Amyotrophic lateral sclerosis (ALS) is an incurable neuromuscular disease that leads to a profound loss of life quality and premature death. Around 10% of the cases are inherited and ALS8 is an autosomal dominant form of familial ALS caused by mutations in the vamp-associated protein B/C (*VAPB*) gene. The VAPB protein is involved in many cellular processes and it likely contributes to the pathogenesis of other forms of ALS besides ALS8. A number of successful drug tests in ALS animal models could not be translated to humans underscoring the need for novel approaches. The induced pluripotent stem cells (iPSC) technology brings new hope, since it can be used to model and investigate diseases *in vitro*. Here we present an additional tool to study ALS based on ALS8-iPSC. Fibroblasts from ALS8 patients and their non-carrier siblings were successfully reprogrammed to a pluripotent state and differentiated into motor neurons. We show for the first time that VAPB protein levels are reduced in ALS8-derived motor neurons but, in contrast to over-expression systems, cytoplasmic aggregates could not be identified. Our results suggest that optimal levels of VAPB may play a central role in the pathogenesis of ALS8, in agreement with the observed reduction of VAPB in sporadic ALS.

INTRODUCTION

Amyotrophic lateral sclerosis (ALS), also known as Lou Gehrig's disease, is the most common adult-onset motor neuron disease (MND) (1). Clinical findings include muscular atrophy and weakness, accompanied by fasciculation and spasticity, and a rapid and progressive degeneration of motor neurons in the cortex, brainstem and spinal cord (2). Patient's death occurs between 2 and 5 years after the symptom onset, usually due to respiratory failure (3). Not only there is no cure for the disease, but its pathogenesis is also poorly understood. Approximately 90% of all ALS cases are sporadic (SALS) and the remaining 10% comprise the familial forms (FALS), most having an autosomal dominant pattern of inheritance (4). More than 10 different loci have

*To whom correspondence should be addressed. Email: muotri@ucsd.edu (A.R.M); mayazatz@usp.br (M.Z.)

been implicated in ALS, including superoxide dismutase 1 (SOD1, ALS1) (5), Tar-DNA-binding protein-43 (TDP-43, ALS10) (6–8), fused sarcoma (FUS, ALS6) (9,10) and vamp-associated protein B/C (VAPB, ALS8) (11).

ALS8 is an autosomal dominant type of FALS that was first mapped in a Brazilian family (12). Subsequently, the mutation c.166C>T in the vesicle-associated membrane protein-associated protein-B/C (*VAPB/C*) gene was identified in the original family and six additional ALS pedigrees in Brazil (11). The pyrimidine transition leads to a substitution of a proline by a serine at position 56 (P56S) of the VAPB protein (11). A founder effect is suggested in the Brazilian families, since they share the same haplotype (13). However, ALS8 is not restricted to South America. The same P56S mutation was identified in Germany (14) and in a patient with Japanese ancestry (15). The German patient harbors a haplotype that is different from the Brazilian families, suggesting that this P56S mutation arose independently from the Brazilian founder mutation (14). Additionally, a recent study found a new mutation (T46I) in a British ALS patient leading to similar molecular defects as the P56S alteration (16). These mutations have not been observed in persons who are not affected by ALS or other MNDs (11,16). Together, these data provide evidence that ALS8 is not as rare as previously proposed (17,18).

ALS8 is associated with a highly variable clinical course. Some affected patients may have a rapid and severe course, while others exhibit a slow progression, and it sometimes takes decades before a severe motor disability develops (11 and unpublished data). Understanding what protects some individuals from the deleterious effect of the VAPB mutation is of great interest since it may provide a window for treatments. VAPB is a type II integral membrane protein comprised of an amino terminal major sperm protein (MSP), a central coiled-coil and an endoplasmatic reticulum membrane anchored carboxy terminal domain (19–21). This protein is phylogenetically well conserved; homologs of VAPB are found across species from yeast to mammals (11,21,22). VAPs are typically ubiquitously expressed and localized to the endoplasmic reticulum and pre-Golgi intermediates (23). They have been implicated in numerous cellular functions, including the regulation of lipid transport and homeostasis, formation of presynaptic terminal and unfolded protein responses (UPRs) (24). VAP was also shown to function as a secreted hormone as the MSP domain of VAP is cleaved, secreted and act as a ligand for Eph receptor in worms and flies (25). Hence, defects in many cellular processes are likely to be involved in the pathogenesis of ALS8. The biological nature of the P56S mutation seems complex. First, the P56S mutation may cause a loss of function as it leads to a reduced level of interaction of VAPB with some key proteins (26). However, mild over-expression of the mutant VAPB has been shown to induce an UPR in cultured cells (27) and flies (25), similar to what has been observed in SOD1 mice (28). These data indicate that it may be toxic, and have gain of function properties. Finally, the mutation may also cause a dominant negative effect since the mutant protein sequesters wild-type (WT) VAPB, contributing to cytoplasmic aggregates (16,21).

Loss of VAPB function may contribute to other familial and sporadic ALS. Indeed, a reduction in VAPB protein levels has been documented in motor neurons from SALS patients (29,30). Moreover, VAPB levels decrease concomitantly with disease's progression in the SOD1 mouse model (29). However, it has not been determined how loss of VAPB is involved in the pathogenesis of sporadic or familial ALS. The study of ALS in human cells may help establish how the loss of VAPB causes the disease but such cells are currently not available. The induced pluripotent stem cell (iPSC) technology provides a new opportunity as it allows ALS patients' genomes to be captured in pluripotent stem cell lineages. Creating iPSC from tissues from ALS patients may also address human-specific effects maintaining the genetic background in which the disease occurs (31). Here, we demonstrate the successful generation of iPSC and further motor neuron differentiation from ALS8 patient cells. We find that the VAPB protein is present in pluripotent stem cells and motor neurons derived from iPSCs. Importantly, we show that the levels of VAPB are reduced in fibroblasts, in iPSCs and motor neurons of ALS8 patients. We propose that reduced levels of VAPB might be an initial defect leading to ALS8 pathogenesis and that ALS8-iPSC could be used to develop early diagnostic tools and to identify possible drugs and targets for future therapies.

RESULTS

Generation of iPSCs from fibroblasts of ALS8 patients

In order to reduce possible differences caused by the genetic background, we chose two ALS8 families and collected skin biopsies from affected patients and their non-carrier siblings, after signing the consent form. Family 1 consists of two non-affected controls and two patients; and Family 2 has one control and two patients (Fig. 1A). We cultured the explants following standard cell culture protocols. We performed cellular reprogramming as described (32), using *c-Myc*, *Oct3/4*, *Klf4* and *SOX2* (31). This allowed the generation of human embryonic stem cell (hESC)-like cells 10–15 days after virus transduction (Fig. 1B and C). We selected iPSC colonies based on hESC-like morphology and transferred them to feeder-free culture conditions (Fig. 1D and E). We successfully reprogrammed all seven samples (four patients and three controls) to iPSCs and expanded them through several passages. We analyzed the C>T166 mutation using polymerase chain reaction (PCR) and *Hae*III restriction enzyme digests that reveal an unique band for the ALS8 mutation, not present in control DNA and confirmed the P56S mutation in all patients derived cells (Supplementary Material, Fig. S1). To determine whether the cells are pluripotent, we carried out immunocytochemistry of iPSC colonies with pluripotent markers. We found that iPSC from control individuals and ALS8 patients expressed both *Lin28* and *Nanog* (Fig. 1F–I). We also performed semi-quantitative RT–PCR using primers for the endogenous expression of *Oct4* and *Nanog* to examine their expression. We found that these markers are present in iPSC but not in fibroblasts from the same individual (Supplementary Material, Fig. S2). More importantly, to confirm if induced iPSCs have pluripotency *in vivo*, we injected them subcutaneously in nude mice to examine whether the iPSCs can induce teratomas. Indeed, we found tissues derived from the three germ layers, including gut-like

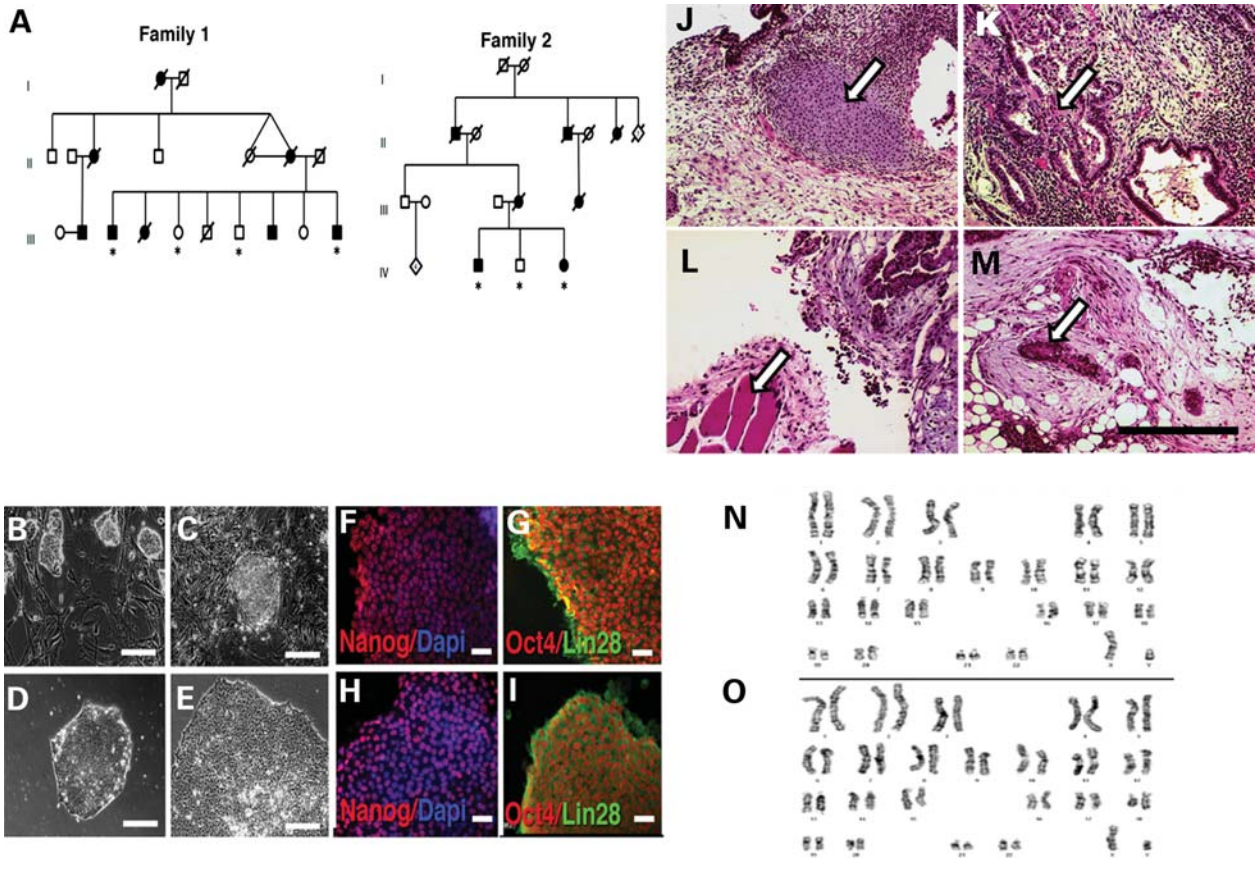

Figure 1. Generation and characterization of controls and ALS8-patients iPSCs. (**A**) Heredograms of the two studied ALS8 families. ALS8 patients are represented in dark symbols and non-affected individuals in white. Skin biopsies were collected (*) from two affected and two control individuals of family 1; and one control and two affected individuals of family 2. (**B**) Phase contrast showing iPSC colony morphology after 1 week post-infection growing in mitotically inactivated mouse embryonic fibroblasts. (**C**) Isolated iPSC colony with similar morphology to hESCs. (**D**) iPSC colony on feeder-free condition. (**E**) Representative image of an established human iPSC colony, with well-defined borders and compact cells. Bar = 100 μm. ALS8-iPSC (**F** and **G**) and WT-iPSC (**H** and **I**) staining, showing the expression of pluripotent markers. Bar = 20 μm. Derived iPSC clones were able to generate teratomas in nude mice. Tissues from the three germ layers could be identified, as shown by arrows: mesoderm: cartilage (**J**) and muscle (**L**); endoderm: gut-like epithelium (**K**); ectoderm: neural rosettes (**M**). Bar = 200 μm. The karyotype from ALS8- (**N**) and WT-iPSCs (**O**) showed normal chromosomal number.

cells from endodermal origin, cartilage and muscle from mesodermal and neural rosettes from ectodermal origin (Fig. 1J–M). To ensure that genomic rearrangements were not induced, we karyotyped the cells. iPSC chromosomal number and organization were normal (Fig. 1N–O). These data collectively suggest that we successfully generated ALS8-iPSCs derived from tissues of ALS8 patients and their normal siblings.

Next, we examined whether WT or ALS8 mutant VAPB is expressed in iPSC cells. Although VAPB is shown to be expressed in many tissues (27), it remains to be established whether it is expressed in pluripotent cells. To detect the VAPB protein specifically, we raised a monoclonal antibody (A1315F3G10) against a sequence in the VAPB N-terminal portion. The sequence is unique for VAPB and the antibody does not recognize the VAPA protein (Supplementary Material, Fig. S3). We confirmed that the monoclonal VAPB antibody can detect expression of WT VAPB and mutant ALS8 in cultured cells expressing WT VAPB and P56S mutant VAPB, respectively (Fig. 2A). Moreover, this antibody is able to detect the cytoplasmic inclusions generated by overexpression of P56S-VAPB (Fig. 2A and inset). We performed immunostaining of ALS8-iPSCs and control iPSCs with anti-VAPB antibody and a pluripotent marker, anti-Nanog antibody. We found that VAPB is expressed in ALS8-iPSCs similar to control iPSCs (Fig. 2B). Cell reprogramming to a pluripotent state requires several steps involving transcriptional and epigenetic factors. To further establish that the VAPB protein is expressed in pluripotent stages, we also examined the expression of VAPB in human ES cells lines, HUES9 and HUES6, by western blotting with anti-VAPB antibody. We found that VAPB is also expressed in both human ES cells (Fig. 2C), suggesting that it is present in cells at pluripotent stages. Taken together, the data indicate that the P56S mutation in iPSCs does not interfere with pluripotency.

P56S VAPB mutation does not inhibit differentiation and maintenance of motor neuron derived from iPSC

To determine whether the motor neurons of ALS8 patients derived from iPSCs display defects, we induced motor neuron differentiation from ALS8-iPSCs and controls based on a previous protocol (33) with minor modifications (see Materials and Methods). To identify motor neurons, we

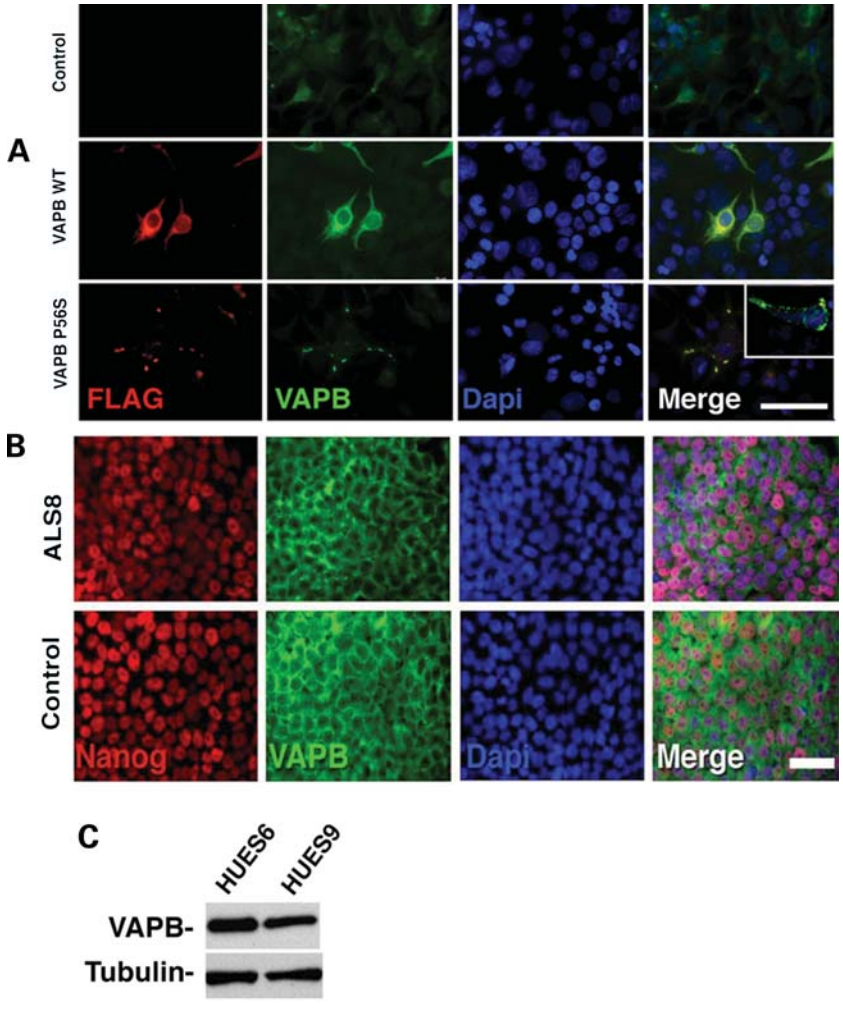

Figure 2. VAPB in human cells. (**A**) Over-expression of WT and P56S forms of VAPB in HEK293T cells. Controls in this experiment were the non-transfected HEK293T cells. While the WT form showed a cytoplasmic distribution with higher intensity around the nucleus, over-expression of mutant protein was mainly localized as cytoplasmic aggregates. Bar = 70 μm. Inset: detail of cytoplasmic inclusions generated by P56S-VAPB over-expression on HEK293T cells. (**B**) VAPB shows perinuclear staining on both WT and ALS8-iPSC expressing the pluripotent marker Nanog. Bar = 50 μm. (**C**) hESCs also express VAPB.

used a reporter construct Hb9 (promoter/enhancer)-GFP (*Hb9*::GFP) (33). We first created embryoid bodies (EBs) in suspension and induced neuronal cells from iPSCs. After 4 weeks of incubation, we confirmed neuronal differentiation by the expression of motor neuron progenitor marker Islet-1 (Fig. 3A) and the postmitotic neuronal marker Map2 (Fig. 3B and C). We then dissociated EBs and plated them on coated dishes. After 7 weeks of differentiation, we observed expression of the *HB9*::GFP reporter, in both control and ALS8-iPSC-derived cells, suggesting the induction of motor neurons from both ALS8-iPSCs and control iPSCs (*D*). Finally, iPSC-derived motor neurons were co-cultured with C2C12 myoblasts and could incorporate α-bungarotoxin, revealing neuromuscular junction formation (Fig. 3E and F). Under these conditions, ALS8-iPSCs could be differentiated into motor neurons with similar efficiency as control-iPSCs, ∼5%, suggesting that P56S mutant VAPB does not inhibit motor neuron differentiation and maintenance (Supplementary Material, Fig. S4).

ALS8 mutation does not cause cytoplasmic inclusions in iPSC-derived motor neurons

Abnormal inclusion of cellular proteins is a common feature of many neurodegenerative diseases. Similarly, cytoplasmic inclusions of ALS8 mutant VAPB are likely to be a key pathological feature of ALS8. In cultured cells (11,29,34–38), flies (21,25,39) and mice (40), expression of mutant VAPB causes cytoplasmic inclusions, which also recruit the WT form into the inclusions (25,29). To determine whether VAPB protein inclusions are early pathological features in ALS8 patients, we performed immunostaining of motor neurons derived from control and ALS8-iPSCs. We used motor neurons maintained for 7 weeks of differentiation. VAPB is expressed diffusely in the cytoplasm of motor neurons derived from ALS8-iPSCs similar to control motor neurons (Fig. 3G and H). In contrast to cells expressing mutant VAPB at high levels (Fig. 2A), we did not observe cytoplasmic inclusions of the VAPB protein in motor neurons.

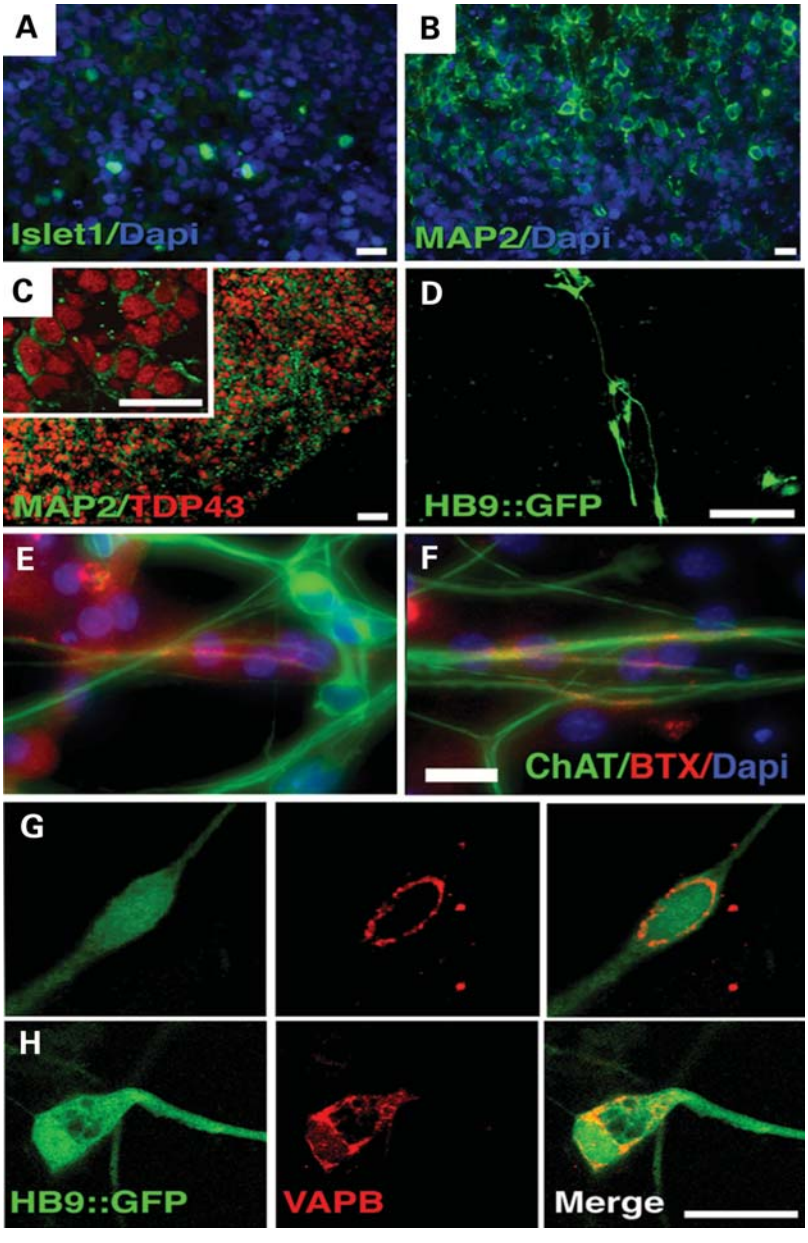

Figure 3. Motor neuron differentiation. (**A**) Expression of the motor neuron progenitor Islet-1 marker in neuroectodermal cells after 4 weeks of differentiation as EB. Bar = 12 μm. (**B**) A mature EB section revealing robust neuronal differentiation, presented by the presence of cells expressing the postmitotic neuronal marker Map2. Bar = 10 μm. (**C**) Cells expressing the mature neuronal marker Map2 also express TDP-43 in the nucleus (inset). Bar = 20 μm. (**D**) Live image of motor neuron-like cells expressing GFP under the control of the *Hb9* promoter. Bar = 100 μm. (**E**) Control and (**F**) ALS8- iPSC-derived motor neurons can incorporate α-bungarotoxin at neuromuscular junctions when co-cultured with C2C12 myoblasts. (**G**) Perinuclear VAPB distribution on a GFP-positive motor neuron derived from a control iPSC clone and (**H**) from an ALS8. Bar = 20 μm.

The P56S mutation causes the VAPB protein to be ubiquitinated (21,34), and ubiquitinated VAP typically accumulates in cytoplasmic inclusions (21). We therefore asked whether increasing levels of VAPB by disturbing the ubiquitin/proteasome system might enhance ubiquitinated VAPB and cytoplasmic aggregates that would not appear under normal cell culture conditions. The proteasome system can be inhibited by the use of a proteasome inhibitor, MG132 (41). We examined ubiquitinated proteins and VAPB inclusions in the presence of MG132 in fibroblasts and motor neurons derived from control and ALS8-iPSCs. In the presence of MG132, we detected an increase in ubiquitin staining in fibroblasts and motor neurons, indicating a successful inhibition of proteasome function (Fig. 4). However, we did not observe an increased accumulation of ubiquitinated protein in ALS8-treated fibroblasts, compared with control cells (Fig. 4A). Similarly, we did not observe increased accumulation of ubiquitinated protein in differentiated motor neurons submitted to MG132 treatment, compared with control cells (Fig. 4B). Surprisingly, both control and ALS8 fibroblasts show reduced VAPB levels after MG132 treatment, suggesting that protein regulatory systems other than the proteasome are acting over VAPB pathway (Fig. 4C).

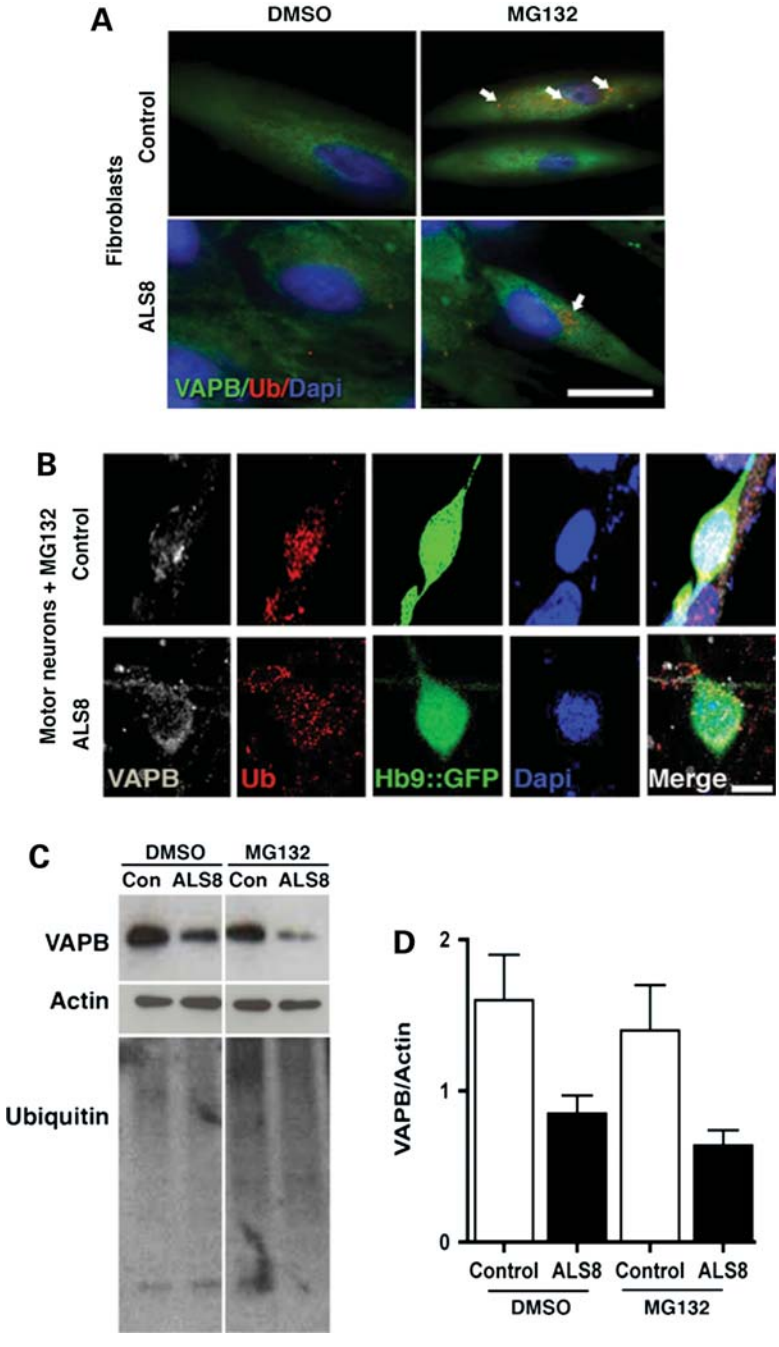

Figure 4. VAPB staining after MG132 treatment. (**A**) Fibroblasts treated with MG132 increased the number of ubiquitin puncta staining (arrows). Bar = 25 μm. (**B**) VAPB perinuclear distribution is similar between control and ALS8-iPSCs-derived *Hb9*::GFP motor neurons after MG132 treatment. Bar = 10 μm. (**C**) Representative data of a western blot for VAPB protein stability after dimethyl sufoxide or MG132 treatment. Higher ubiquitin staining in MG132 lanes shows that proteasome was inhibited. (**D**) Graph represents the average of VAPB protein amount after treatment from two individual controls and two ALS8 patients from the two families.

A failure of upregulation of VAPB protein during motor neuron induction

We sought to determine whether the levels of VAPB protein in ALS8-iPSCs and motor neurons differ in patients when compared with controls. Interestingly, there is a reduction in the levels of VAPB protein in ALS8-iPSCs when compared with control iPSCs (Fig. 5A and B). The reduction in VAPB protein levels is consistently observed independent of the iPSC clone used for comparison (Supplementary Material, Fig. S5). We then examined whether the decreased levels of VAPB protein are also observed during induction of motor neurons. We performed immunoblotting analysis and compared VAPB levels in control and ALS8-iPSC-derived lineages. As shown in Figure 5C and D, in all stages of differentiation, VAPB is significantly reduced in cells derived from

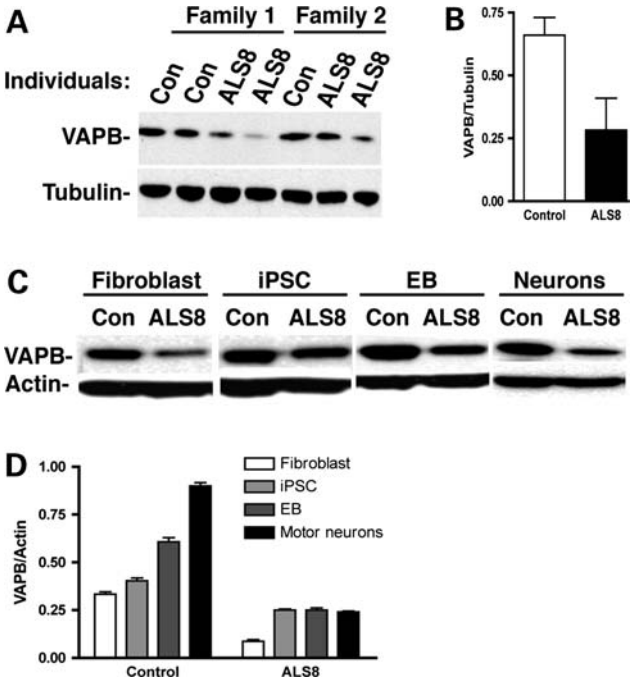

Figure 5. Reduction in VAPB protein levels in ALS8-derived motor neurons. (**A** and **B**) VAPB levels on iPSC lines are reduced on ALS8 samples when compared with controls (Con). (**C**) Reduced levels of VAPB in ALS8 cells during differentiation. (**D**) VAPB increases during motor neuron differentiation of control but not from ALS8-iPSC. $n = 3$ independent experiments.

ALS8-iPSCs. Interestingly, the levels of VAPB protein gradually increase during the differentiation process of control iPSCs (Fig. 5D). However, we did not observe the upregulation of VAPB protein during neuronal differentiation of ALS8-iPSCs (Fig. 5D), suggesting that the ALS8 mutation causes a failure of upregulation of VAPB protein during neuronal and motor neuron inductions. To determine whether the amount of VAPB protein is controlled at the transcriptional level, we performed a real-time PCR analysis. VAPB mRNA levels do not differ between control and ALS8 fibroblast cultures, suggesting that the VAPB regulation is likely to happen at the post-translational level (Supplementary Material, Fig. S6).

DISCUSSION

ALS is a fatal condition whose pathogenesis is still poorly understood. The generation of familial ALS mouse models, especially SOD1, has helped clarify several important aspects of the disease pathogenesis, but a precise molecular mechanism is still lacking. Importantly, several drug tests that were somewhat successful in animal systems were not successfully translated into humans (42). The lack of success of translating these strategies in ALS patients may be due to the use of a single animal model, namely SOD1 mice that carry a high transgene copy number (42,43). Hence, there is a need to create other mouse models as well as strategies to test drugs. The ALS8-associated neurodegeneration pathway seems to share common traits with other ALS forms (29) and the observation that the VAPB protein levels are decreased in sporadic patients so far suggests that it may play an important role in the pathogenesis of numerous forms of the disease (29,30). Thus, we decided to produce ALS8 patient-derived iPSCs as well as iPSCs from their non-carrier siblings as controls.

All fibroblast samples were reprogrammed to a pluripotent status. Their cellular and molecular characterization documents that these are bona fide iPSC. We found no obvious alterations in the VAPB distribution pattern of control and ALS8 cells, and it was not possible to identify inclusions in ALS8-derived motor neurons even after the 7–8 weeks required for neuronal maturation. In addition, the use of the proteasome inhibitor MG132 did not exacerbate the lack of aggregation. This failure to detect aggregates extended to all cell types—fibroblasts, iPSC and cells induced to differentiate into motor neuron. It is important to note that transgenic mutant VAPB mice do not develop MND, although cytoplasmic inclusions appear when they are ~18 months old (40). It is possible that the short longevity of the motor neurons *in vitro* may not permit detection of aggregates in our system. Intracytoplasmic aggregates are found in many different forms of ALS, including SOD1 (ALS1) (44,45), TDP-43 (ALS10) (6–8), FUS/TLS (ALS6) (9) and VAPB itself (11,21,25,29,34–40). Many of the aggregates are also immunopositive for TDP-43. However, they are not found in SOD1 models (46) nor have they been documented in transgenic mice carrying the A315T mutation of the TDP-43 protein (47). Hence, it is not obvious how these aggregates relate to the pathogenesis. It is possible that the neurotoxicity is not due to cytoplasmic inclusions itself (47).

We showed that VAPB is expressed early in development in pluripotent stem cells and that the protein levels increase during motor neuron differentiation. Similar to other studies (48,49), our results suggest that mutations that cause MNDs are unlikely to affect cell reprogramming. This even seems to be the case when the affected protein is expressed in pluripotent stages, as for VAPB (this work) and the SMN protein, responsible for spinal muscular atrophy (48). The importance of VAPB levels has been documented in *Drosophila* neuromuscular junctions. Over-expression of the VAPB orthologue, dVAP-33, in flies reduces the size of boutons at neuromuscular junctions and increases their number, while a reduction or loss of dVAP33 causes a reduction in number and an increase in bouton size (50). The significant reduction in VAPB protein levels especially in motor neurons of ALS8 patients compared with their non-carrier siblings may therefore have biological consequences. The reduction in VAPB is >50% in ALS8 cells when compared with controls. Since VAPB transcript amounts are very similar between control and ALS8 patients' samples, we propose that its expression is regulated at the protein level. The reduction in the VAPB protein after MG132 treatment is in agreement with the absence of aggregates in immunocytochemistry. Accordingly, blocking the ubiquitin pathway did not rescue VAPB levels. Once VAPB reduction is also observed in fibroblasts, these cells could become an alternative source to evaluate strategies aiming the correction of the VAPB's mutant phenotype. There are several possible explanations for VAPB protein reduction in ALS8 patients. The mutant protein may not be properly folded and is less

stable (51,52). Alternatively, it may be that the mutant chain forms a dimer with the wild-type isoforms (38,53), destabilizing the wild-type protein as well. This would imply that the ALS8 mutation functions as a dominant negative allele, and should share features with null alleles, as previously documented (36). Additionally, expression of P56SVAPB shows similar effects as of VAP knockdown on primary neurons, since both induce cell death (29). Results from our work and others (29,36) support the hypothesis that P56S dominant effect is, at least in part, due to VAPB loss of function.

The reduction in VAPB ratio levels between patients and controls enforces the idea that iPSC technology can recapitulate the patients' original cell status (32,54,55). The fact that VAPB is reduced in motor neurons from ALS8 patient's samples suggests that the correct amount of VAPB may be crucial for their survival. The decreased VAPB protein levels in sporadic ALS postmortem tissue and the concomitant reduction in this protein with ALS progression in SOD1 mutant mice strengthen this hypothesis (29). Interestingly, concomitantly with neuronal differentiation, WT cultured cells present an increment of VAPB levels not observed in the mutant cultures. It is known that VAPB processing is different in certain brain regions and during development (27,53). We hypothesize that, even in the presence of a smaller amount of VAPB, ALS8 carriers are normal until they reach the fourth or fifth decade of life, when the levels become critically low. Our results indicate that the iPSCs can recapitulate some aspects of ALS8 and be used to extract new biological information relevant to human motor neuron development. We believe this cellular model has the potential to complement other human and animal models to accelerate the discovery of new compounds for treating ALS and other forms of motor neuron neurodegeneration.

MATERIALS AND METHODS

Skin biopsy

All procedures were conducted with the approval of committees from University of São Paulo (USP, Brazil), Federal University of São Paulo (UNIFESP, Brazil) and University of California San Diego (UCSD). ALS8 patients were analyzed by experienced neurologists that defined the diseases based on clinical findings. Initially, DNA was extracted from lymphocytes. The mutation c.C>T_{166} (P56S) was confirmed by *Hae*III enzyme digestion and by the sequencing of the amplicon containing the exon 2 (11). ALS8 families were selected according to the availability to meet the criteria of a minimum of two affected and one normal sibling from the same genitors. Skin biopsies were performed by a neurologist, using a 3 mm punch, after local anesthesia. Explants were collected in Dulbecco's modified eagle medium (DMEM) (1×) with 5% (v/v) antibiotics (Pen/Strep 10 000 U/ml). Fibroblast cell culture was implemented using DMEM (1×) with 10% (v/v) fetal bovine serum and 2% (v/v) antibiotics.

Cellular reprogramming

Cellular reprogramming was performed as previously described (32). Briefly, the four Yamanaka factors (*c-Myc*, *Oct3/4*, *Klf4* and *SOX2*) (31) in a retrovirus system were used to infect fibroblasts at low passage. After 2 days, infected human fibroblasts were moved to hESC conditions on a feeder layer of irradiated mouse embryonic fibroblasts (Chemicon). hESC-like cells appear 10–15 days after virus transduction. iPSC colonies were selected by morphology and manually moved to a feeder-free condition in Matrigel-coated dishes (BD Bioscience) and mTeSR1 (Stem Cell Techonologies). iPSCs were manually passed and maintained on feeder-free condition until the beginning of the differentiation protocol. Three clones from one control and from two patients were selected for further characterization for each family.

Teratoma formation

Approximately 3×10^6 iPSCs were injected subcutaneously into the dorsal flanks of nude mice (CByJ.Cg-Foxn1 nu/J) anesthetized with isoflurane. Five to 6 weeks after injection, teratomas were dissected, fixed overnight in 10% formalin phosphate and embedded in paraffin. Sections were stained with hematoxylin and eosin for further analysis. Protocols were previously approved by the University of California San Diego Institutional Animal Care and Use Committee.

Motor neuron differentiation

Motor neuron differentiation was based on previous protocol (33) with some modifications. Briefly, the differentiation comprised a period of 7–8 weeks, with 5% efficiency at the end from both control and patients' samples. Confluent iPSC on feeder-free condition was moved to N2 media on F12/DMEM (Invitrogen, Carlsbad, CA, USA), on day 0. On the following day, a BMP signaling inhibitor, dorsomorphin—1 μM (Calbiochem), was added. On the third day, colonies were dissociated using dispase (0.5 mg/ml) and kept under rotation at 37°C to form EBs. Cells were maintained in this condition for 4 more weeks with the gradual addition of neuronal survival and differentiation inducers as follows: day 9, addition of differentiation retinoic acid (1 μM) and ascorbic acid (200 ng/ml) were added; day 16, addition of sonic hedgehog (SHH—500 ng/ml: R&D Systems), brain-derived neural factor (20 ng/ml: Peprotech), growth-derived neural factor (20 ng/ml: Peprotech) with the simultaneous dorsomophin removal. On day 30, cells were plated on poli-ornitine/laminin-coated plates and kept in culture for additional 3–4 weeks. After cell platting, the previous neural induction media were modified by the reduction of SHH to 100 ng/ml and addition of cyclic adenosine monophosphate (1 μM). *Hb9*::GFP reporter construct was transferred to the cells using a lentivirus system (33). The lentivirus was added to the culture either at the dissociation moment or 2 days after plating the cells on poli-O/L. For neuromuscular junction assays, we used C2C12 myoblasts (ATCC) as previously described (33). Briefly, motor neuron progenitors were plated on top of the myotubes for ∼4 weeks. Cells were fixed, and the formation of neuromuscular junctions detected by incorporation of α-bungarotoxin conjugated with Alexa 568 (1:200, Molecular Probes, Invitrogen).

Proteasome inhibition assay

MG132 (Sigma) was used to block the proteasome system. Several attempts were made to optimize the MG132 concentrations. Fibroblasts were kept for 24 h with 10 μM of MG132. Motor neurons were treated with 5 μM of the inhibitor for 24 h.

Karyotyping

Standard G-banding chromosome analysis was performed by Cell Line Genetics (Madison, WI, USA) and Molecular Diagnostic Services, Inc (San Diego, CA, USA).

Immunocytochemistry

Cells were fixed with 4% paraformaldehyde, followed by permeabilization and blocking with 0.1% (v/v) Triton X in PBS containing 5% (v/v) donkey serum, for 1 h. Primary antibodies were incubated overnight at 4°C. Samples were washed three times before secondary antibodies incubation (Jackson Laboratories and Alexa Fluor Dyes, Life Technologies) for 1 h. Primary antibody concentrations were: α-hVAPB mouse monoclonal A1315F3G10 1:500; α-ubiquitin rabbit polyclonal 1:1000 (Dako); α-nanog mouse monoclonal 1:100 (BD Bioscience); α-Oct3/4 mouse monoclonal 1:250 (Santa Cruz); α-Lin28 goat polyclonal 1:400 (R&D Systems); α-MAP2 mouse polyclonal 1:200 (Milipore); α-TDP-43 rabbit polyclonal 1:500 (Novus Biologicals); α-GFP chicken polyclonal 1:500 (Aves Lab) and α-ChAt 1:100 (Chemicon). Images were obtained trough Olympus FV1000 confocal microscope and Zeiss immunofluorescence microscope.

Western blot analysis

Cells were collected, re-suspended in 1× RIPA lyses buffer (Milipore) containing 1% (v/v) protein inhibitor cocktail (Sigma), triturated and centrifuged at 10 000*g* for 20 min at 4°C. Ten micrograms of protein extract were separated in a 4–12% pre-cast Bis–Tris acrylamide gradient gel (Invitrogen, Life Tech), transferred to a nitrocellulose membrane and probed with primary antibodies: α-hVAPB mouse monoclonal A1315F3G10 1:1000, or α-ubiquitin rabbit polyclonal 1:1000 (Dako), followed by horseradish peroxidase-conjugated secondary antibody. Visualization was made by ECL chemiluminescence (Amersham). Membranes were striped and re-probed using antibodies against β-actin 1:5000 (Ambion) and tubulin 1:5000 (Ambion) to generate a control for protein loading. For semi-quantitative analysis, films were scanned with Typhoon 8600 scanner (Molecular Dynamics) and band signal intensity was analyzed and corrected with respect to tubulin and β-actin using ImageJ.

RNA extraction and RT–PCR

Total RNA was extracted using Trizol. Reverse transcriptase reaction was performed by the use of Super Script III First-Strand Synthesis System for RT–PCR from Invitrogen. cDNA synthesis was amplified by PCR using the following primers: *Nanog F* 5′-cctatgcctgtgatttgtgg-3′ and *Nanog R* 5′-ctgggaccttgtcttccttt-3′; h*Oct4 F* 5′-gggaggggaggagctagg-3′ and h*Oct4 R* 5′-tccaaccagttgccccaaac-3′. We performed real-time PCR with SYBR Green Mix and using primers for GAPDH *F* 5′-TGCACCACCAACTGCTTAGC-3′ and *R* 5′-ggcatggactgtggtcatg-3′; VAPB *F* 5′-ccaatagtgtctaagtctctgag-3′ and *R* 5′-gtccatcttcttccttgaactg-3′ on 7500 Real-Time PCR System (Applied Biosystems/Life Tech). Results were extracted and analyzed using 7500 Software v2.0.4.

SUPPLEMENTARY MATERIAL

Supplementary Material is available at *HMG* online.

ACKNOWLEDGEMENTS

We would like to thank Dr Johnny Ngsee for providing VAP plasmids.

Conflict of Interest statement. None declared.

FUNDING

The work was supported by the Fundação de Amparo à Pesquisa do Estado de São Paulo—Centro de Estudos do Genoma Humano (FAPESP-CEPID); Instituto Nacional de células-tronco em doenças genéticas (INCT); Conselho Nacional de Desenvolvimento Científico e Tecnológico (CNPq); Muscular Dystrophy Association Grant (MDA185410) and Instituto Paulo Gontijo (IPG). Funding to pay the Open Access publication charges for this article was provided by FAPESP-CEPID and INCT.

REFERENCES

1. Goodall, E.F. and Morrison, K.E. (2006) Amyotrophic lateral sclerosis (motor neuron disease): proposed mechanisms and pathways to treatment. *Expert. Rev. Mol. Med.*, **8**, 1–22.
2. Rowland, L.P. and Shneider, N.A. (2001) Amyotrophic lateral sclerosis. *N. Engl. J. Med.*, **344**, 1688–1700.
3. Beleza-Meireles, A. and Al-Chalabi, A. (2009) Genetic studies of amyotrophic lateral sclerosis: controversies and perspectives. *Amyotroph. Lateral Scler.*, **10**, 1–14.
4. Pasinelli, P. and Brown, R.H. (2006) Molecular biology of amyotrophic lateral sclerosis: insights from genetics. *Nat. Rev. Neuron.*, **7**, 710–723.
5. Rosen, D.R., Siddique, T., Patterson, D., Figlewicz, D.A., Sapp, P., Hentati, A., Donaldson, D., Goto, J., O'Regan, J.P., Deng, H.X. *et al.* (1993) Mutations in Cu/Zn superoxide dismutase gene are associated with familial amyotrophic lateral sclerosis. *Nature*, **362**, 59–62.
6. Gitcho, M.A., Baloh, R.H., Chakraverty, S., Mayo, K., Norton, J.B., Levitch, D., Hatanpaa, K.J., White, C.L. 3rd, Bigio, E.H., Caselli, R. *et al.* (2008) TDP-43 A315T mutation in familial motor neuron disease. *Ann. Neurol.*, **63**, 535–538.
7. Sreedharan, J., Blair, I.P., Tripathi, V.B., Hu, X., Vance, C., Rogelj, B., Ackerley, S., Durnall, J.C., Williams, K.L., Buratti, E. *et al.* (2008) TDP-43 mutations in familial and sporadic amyotrophic lateral sclerosis. *Science*, **319**, 1668–1672.
8. Kabashi, E., Valdmanis, P.N., Dion, P., Spiegelman, D., McConkey, B.J., Vande Velde, C., Bouchard, J.P., Lacomblez, L., Pochigaeva, K., Salachas, F. *et al.* (2008) TARDBP mutations in individuals with sporadic and familial amyotrophic lateral sclerosis. *Nat. Genet.*, **40**, 572–574.
9. Vance, C., Rogelj, B., Hortobágyi, T., De Vos, K.J., Nishimura, A.L., Sreedharan, J., Hu, X., Smith, B., Ruddy, D., Wright, P. *et al.* (2009) Mutations in FUS, an RNA processing protein, cause familial amyotrophic lateral sclerosis type 6. *Science*, **323**, 1208–1211.

10. Kwiatkowski, T.J. Jr, Bosco, D.A., Leclerc, A.L., Tamrazian, E., Vanderburg, C.R., Russ, C., Davis, A., Gilchrist, J., Kasarskis, E.J., Munsat, T. *et al.* (2009) Mutations in the FUS/TLS gene on chromosome 16 cause familial amyotrophic lateral sclerosis. *Science*, **323**, 1205–1208.
11. Nishimura, A.L., Mitne-Neto, M., Silva, H.A.C., Richieri-Costa, A., Middleton, S., Cascio, D., Kok, F., Oliveira, J.R., Gillingwater, T., Webb, J., Skehel, P. and Zatz, M. (2004) A mutation in the vesicle-trafficking protein VAPB causes late-onset spinal muscular atrophy and amyotrophic lateral sclerosis. *Am. J. Hum. Genet.*, **75**, 822–831.
12. Nishimura, A.L., Mitne-Neto, M., Silva, H.C.A., Oliveira, J.R.M., Vainzof, M. and Zatz, M. (2004) A novel locus for a late onset amyotrophic lateral sclrerosis/motor neuron disease (ALS/MND) variant at 20q13. *J. Med. Genet.*, **41**, 315–320.
13. Nishimura, A.L., Al-Chalabi, A. and Zatz, M. (2007) A common founder for amyotrophic lateral sclerosis type 8 (ALS8) in the Brazilian population. *Hum. Genet.*, **118**, 499–500.
14. Funke, A.D., Esser, M., Krüttgen, A., Weis, J., Mitne-Neto, M., Lazar, M., Nishimura, A.L., Sperfeld, A.D., Trillenberg, P., Senderek, J. *et al.* (2010) The p.P56S mutation in the VAPB gene is not due to a single founder: the first European case. *Clin. Genet.*, **77**, 302–303.
15. Millecamps, S., Salachas, F., Cazeneuve, C., Gordon, P., Bricka, B., Camuzat, A., Guillot-Noël, L., Russaouen, O., Bruneteau, G., Pradat, P.F. *et al.* (2010) SOD1, ANG, VAPB, TARDBP, and FUS mutations in familial amyotrophic lateral sclerosis: genotype-phenotype correlations. *J. Med. Genet.*, **47**, 554–560.
16. Chen, H.J., Anagnostou, G., Chai, A., Withers, J., Morris, A., Adhikaree, J., Pennetta, G. and de Belleroche, J.S. (2010) Characterization of the properties of a novel mutation in VAPB in familial amyotrophic lateral sclerosis. *J. Biol. Chem.*, **285**, 40266–40281.
17. Hirano, M. (2008) VAPB: new genetic clues to the pathogenesis of ALS. *Neurology*, **70**, 1161–1162.
18. Landers, J.E., Leclerc, A.L., Shi, L., Virkud, A., Cho, T., Maxwell, M.M., Henry, A.F., Polak, M., Glass, J.D., Kwiatkowski, T.J. *et al.* (2008) New VAPB deletion variant and exclusion of VAPB mutations in familial ALS. *Neurology*, **70**, 1179–1185.
19. Weir, M.L., Klip, A. and Trimble, W.S. (1998) Identification of a human homologue of the vesicle-associated membrane protein (VAMP)-associated protein of 33 kDa (VAP-33): a broadly expressed protein that binds to VAMP. *Biochem. J.*, **333**, 247–251.
20. Nishimura, Y., Hayashi, M., Inada, H. and Tanaka, T. (1999) Molecular cloning and characterization of mammalian homologues of vesicle-associated membrane protein-associated (VAMP-associated) proteins. *Biochem. Biophys. Res. Commun.*, **254**, 21–26.
21. Ratnaparkhi, A., Lawless, G.M., Schweizer, F.E., Golshani, P. and Jackson, G.R. (2008) A Drosophila model of ALS: human ALS-associated mutation in VAP33A suggests a dominant negative mechanism. *PLoS ONE*, **3**, e2334.
22. Kaiser, S.E., Brickner, J.H., Reilein, A.R., Fenn, T.D., Walter, P. and Brunger, A.T. (2005) Structural basis of FFAT motif-mediated ER targeting. *Structure*, **13**, 1035–1045.
23. Skehel, P., Fabian-Fine, R. and Kandel, E. (2000) Mouse VAP33 is associated with the endoplasmic reticulum and microtubules. *Proc. Natl Acad. Sci. USA*, **97**, 1101–1106.
24. Lev, S., Halevy, D.B., Peretti, D. and Dahan, N. (2008) The VAP protein family: from cellular functions to motor neuron disease. *Trends Cell Biol.*, **18**, 282–290.
25. Tsuda, H., Han, S.M., Yang, Y., Tong, C., Lin, Y.Q., Mohan, K., Haueter, C., Zoghbi, A., Harati, Y., Kwan, J., Miller, M.A. and Bellen, H.J. (2008) The amyotrophic lateral sclerosis 8 protein VAPB is cleaved, secreted, and acts as a ligand for Eph receptors. *Cell*, **133**, 963–977.
26. Mitne-Neto, M., Ramos, C.R., Pimenta, D.C., Luz, J.S., Nishimura, A.L., Gonzales, F.A., Oliveira, C.C. and Zatz, M. (2007) A mutation in human VAP-B–MSP domain, present in ALS patients, affects the interaction with other cellular proteins. *Protein Expr. Purif.*, **55**, 139–146.
27. Gkogkas, C., Middleton, S., Kremer, A.M., Wardrope, C., Hannah, M., Gillingwater, T.H. and Skehel, P. (2008) VAPB interacts with and modulates the activity of ATF6. *Hum. Mol. Genet.*, **17**, 1517–1526.
28. Wang, L., Popko, B. and Roos, R.P. (2011) The unfolded protein response in familial amyotrophic lateral sclerosis. *Hum. Mol. Genet.*, **20**, 1008–1015.
29. Teuling, E., Ahmed, S., Haasdijk, E., Demmers, J., Steinmetz, M.O., Akhmanova, A., Jaarsma, D. and Hoogenraad, C.C. (2007) Motor neuron disease-associated mutant vesicle-associated membrane protein-associated protein (VAP) B recruits wild-type VAPs into endoplasmic reticulum-derived tubular aggregates. *J. Neurosci.*, **27**, 9801–9815.
30. Anagnostou, G., Akbar, M.T., Paul, P., Angelinetta, C., Steiner, T.J. and de Belleroche, J. (2010) Vesicle associated membrane protein B (VAPB) is decreased in ALS spinal cord. *Neurobiol. Aging*, **31**, 969–985.
31. Takahashi, K., Tanabe, K., Ohnuki, M., Narita, M., Ichisaka, T., Tomoda, K. and Yamanaka, S. (2007) Induction of pluripotent stem cells from adult human fibroblasts by defined factors. *Cell*, **13**, 861–872.
32. Marchetto, M.C., Carromeu, C., Acab, A., Yu, D., Yeo, G.W., Mu, Y., Chen, G., Gage, F.H. and Muotri, A.R. (2010) A model for neural development and treatment of Rett syndrome using human induced pluripotent stem cells. *Cell*, **143**, 527–539.
33. Marchetto, M.C., Muotri, A.R., Mu, Y., Smith, A.M., Cezar, G.G. and Gage, F.H. (2008) Non-cell-autonomous effect of human SOD1 G37R astrocytes on motor neurons derived from human embryonic stem cells. *Cell Stem Cell*, **3**, 649–657.
34. Kanekura, K., Nishimoto, I., Aiso, S. and Matsuoka, M. (2006) Characterization of amyotrophic lateral sclerosis-linked P56S mutation of vesicle-associated membrane protein-associated protein B (VAPB/ALS8). *J. Biol. Chem.*, **28**, 30223–30232.
35. Prosser, D.C., Tran, D., Gougeon, P.Y., Verly, C. and Ngsee, J.K. (2008) FFAT rescues APA-mediated inhibition of ER-to-Golgi transport and VAPB-mediated ER aggregation. *J. Cell Sci.*, **12**, 3052–3061.
36. Suzuki, H., Kanekura, K., Levine, T.P., Kohno, K., Olkkonen, V.M., Aiso, S. and Matsuoka, M. (2009) ALS-linked P56S-VAPB, an aggregated loss-of-function mutant of VAPB, predisposes motor neurons to ER stress-related death by inducing aggregation of co-expressed wild-type VAPB. *J. Neurochem.*, **108**, 973–985.
37. Fasana, E., Fossati, M., Ruggiano, A., Brambillasca, S., Hoogenraad, C.C., Navone, F., Francolini, M. and Borgese, N. (2010) A VAPB mutant linked to amyotrophic lateral sclerosis generates a novel form of organized smooth endoplasmic reticulum. *FASEB*, **24**, 1419–1430.
38. Kim, S., Leal, S., Halevy, D.B., Gomes, M. and Lev, S. (2010) Structural requirements for VAP-B oligomerization and their implication in amyotrophic lateral sclerosis-associated. *J. Biol. Chem.*, **285**, 13839–13849.
39. Chai, A., Withers, J., Koh, Y.H., Parry, K., Bao, H., Zhang, B., Budnik, V. and Pennetta, G. (2008) hVAPB, the causative gene of a heterogeneous group of motor neuron diseases in humans, is functionally interchangeable with its Drosophila homologue DVAP-33A at the neuromuscular junction. *Hum. Mol. Genet.*, **17**, 266–280.
40. Tudor, E.L., Galtrey, C.M., Perkinton, M.S., Lau, K.F., De Vos, K.J., Mitchell, J.C., Ackerley, S., Hortobágyi, T., Vámos, E., Leigh, P.N. *et al.* (2010) Amyotrophic lateral sclerosis mutant vesicle-associated membrane protein- associated protein-B transgenic mice develop TAR-DNA-binding protein-43 pathology. *Neuroscience*, **167**, 774–785.
41. Joazeiro, C.A.P., Anderson, K.C. and Hunter, T. (2006) Proteasome inhibitor drugs on the rise. *Cancer Res.*, **16**, 7840–7842.
42. Ludolph, A.C., Bendotti, C., Blaugrund, E., Chio, A., Greensmith, L., Loeffler, J.P., Mead, R., Niessen, H.G., Petri, S., Pradat, P.F. *et al.* (2010) Guidelines for preclinical animal research in ALS/MND: A consensus meeting. *Amyotroph. Lateral Scler.*, **11**, 38–45.
43. Pizzasegola, C., Caron, I., Daleno, C., Ronchi, A., Minoia, C., Carrì, M.T. and Bendotti, C. (2009) Treatment with lithium carbonate does not improve disease progression in two different strains of SOD1 mutant mice. *Amyotroph. Lateral Scler.*, **10**, 221–228.
44. Bruijn, L.I., Becher, M.W., Lee, M.K., Anderson, K.L., Jenkins, N.A., Copeland, N.G., Sisodia, S.S., Rothstein, J.D., Borchelt, D.R., Price, D.L. and Cleveland, D.W. (1997) ALS-linked SOD1 mutant G85R mediates damage to astrocytes and promotes rapidly progressive disease with SOD1-containing inclusions. *Neuron*, **18**, 327–338.
45. Bergemalm, D., Forsberg, K., Srivastava, V., Graffmo, K.S., Andersen, P.M., Brännström, T., Wingsle, G. and Marklund, S.L. (2010) Superoxide dismutase-1 and other proteins in inclusions from transgenic amyotrophic lateral sclerosis model mice. *J. Neurochem.*, **114**, 408–418.
46. Lagier-Tourenne, C. and Cleveland, D.W. (2009) Rethinking ALS: the FUS about TDP-43. *Cell*, **136**, 1001–1004.
47. Wegorzewska, I., Bell, S., Cairns, N.J., Miller, T.M. and Baloh, R.H. (2009) TDP-43 mutant transgenic mice develop features of ALS and frontotemporal lobar degeneration. *Proc. Natl Acad. Sci. USA*, **106**, 18809–18814.

48. Ebert, A.D., Yu, J., Rose, F.F. Jr, Mattis, V.B., Lorson, C.L., Thomson, J.A. and Svendsen, C.N. (2009) Induced pluripotent stem cells from a spinal muscular atrophy patient. *Nature*, **457**, 277–280.
49. Dimos, J.T., Rodolfa, K.T., Niakan, K.K., Weisenthal, L.M., Mitsumoto, H., Chung, W., Croft, G.F., Saphier, G., Leibel, R., Goland, R. *et al.* (2008) Induced pluripotent stem cells generated from patients with ALS can be differentiated into motor neurons. *Science*, **321**, 1218–1221.
50. Pennetta, G., Hiesinger, P.R., Fabian-Fine, R., Meinertzhagen, I.A. and Bellen, H.J. (2002) Drosophila VAP-33A directs bouton formation at neuromuscular junctions in a dosage-dependent manner. *Neuron*, **35**, 291–306.
51. Shi, J., Lua, S., Tong, J.S. and Song, J. (2010) Elimination of the native structure and solubility of the hVAPB MSP domain by the Pro56Ser mutation that causes amyotrophic lateral sclerosis. *Biochemistry*, **49**, 3887–3897.
52. Furuita, K., Jee, J., Fukada, H., Mishima, M. and Kojima, C. (2010) Electrostatic interaction between oxysterol-binding protein and VAMP-associated protein A revealed by NMR and mutagenesis studies. *J. Biol. Chem.*, **285**, 12961–12970.
53. Gkogkas, C., Wardrope, C., Hannah, M. and Skehel, P. (2011) The ALS8-associated mutant VAPB(P56S) is resistant to proteolysis in neurons. *J. Neurochem.* doi: 10.1111/j.1471–4159.2011.07201.
54. Marchetto, M.C.N., Winner, B. and Gage, F.H. (2010) Pluripotent stem cells in neurodegenerative and neurodevelopmental diseases. *Hum. Mol. Genet.*, **19**, R71–R76.
55. Park, I.H., Arora, N., Huo, H., Maherali, N., Ahfeldt, T., Shimamura, A., Lensch, M.W., Cowan, C., Hochedlinger, K. and Daley, G.Q. (2008) Disease-specific induced pluripotent stem (iPS) cells. *Cell*, **134**, 877–886.